Neuroscience 274 (2014) 273–288

INCREASED EXPRESSION OF AQUAPORIN 4 IN THE RAT HIPPOCAMPUS AND CORTEX DURING TRIMETHYLTIN-INDUCED NEURODEGENERATION

S. CECCARIGLIA,[a] A. D'ALTOCOLLE,[a] A. DEL FA',[a] A. SILVESTRINI,[b] M. BARBA,[a] F. PIZZOLANTE,[a] A. REPELE,[c] F. MICHETTI[a]* AND C. GANGITANO[a]

[a] *Institute of Anatomy and Cell Biology, Università Cattolica del Sacro Cuore, L. go F. Vito 1, 00168 Rome, Italy*

[b] *Institute of Biochemistry and Clinical Chemistry, Università Cattolica del Sacro Cuore, L. go F. Vito 1, 00168 Rome, Italy*

[c] *Institute Pasteur de Lille, Lille2 University, rue du Professeur Laguesse, 59000 Lille, France*

Abstract—Trimethyltin chloride (TMT) is a neurotoxicant producing neuronal degeneration and reactive astrogliosis in the mammalian central nervous system, especially the hippocampus. A previous magnetic resonance imaging investigation in TMT-treated rats evidenced dilation of lateral ventricles, also suggesting alterations in blood–brain barrier permeability and brain edema. Aquaporin 4 (AQP4), a glial water channel protein expressed mainly in the nervous system, is considered a specific marker of vascular permeability and thought to play an important role in brain edema (conditions). We studied AQP4 expression in the hippocampus and cerebral cortex of TMT-treated rats in order to explore the molecular mechanisms involved in brain edema occurring in these experimental conditions. Real-time PCR and western blotting data showed significant up-regulation of both AQP4 mRNA and protein levels starting 14 days after TMT treatment in the hippocampus and cortex. Parallel immunofluorescence studies indicated intense astrogliosis and AQP4 immunoreactivity diffusely pronounced in the hippocampal and cortex areas starting 14 days after TMT intoxication. In order to study the effects of TMT on vascular integrity, double-label immunofluorescence experiments for rat immunoglobulin G (IgG) and rat endothelial cell antigen-1 (RECA-1) or neuronal nuclei (NeuN) (endothelial and neuronal markers respectively) were performed. The results indicated, at 21 and 35 days after treatment, the presence of rat IgG in paravasal parenchyma and in some neuronal cells of the hippocampus and cortex. The extravasated IgG staining was temporally correlated with over-expression of neuronal vascular endothelial growth factor (VEGF) and the active phosphorylated form of its neuronal receptor (VEGFR-2P), suggesting that these factors may cooperate in mediating vascular leakage.
© 2014 IBRO. Published by Elsevier Ltd. All rights reserved.

Key words: trimethyltin, hippocampus, cortex, Aquaporin 4, vascular endothelium growth factor, neurodegeneration.

INTRODUCTION

Trimethyltin chloride (TMT) is a well characterized neurotoxicant. It is a by-product in the manufacture of dimethyltin chloride, commonly used in both industrial and agricultural settings.

TMT intoxication produces significant, selective neuronal death in the rodent limbic system, especially in the CA1 and CA3/CA4 subfields of the hippocampus, but also in layer II of the piriform/entorhinal cortex and in the pyramidal cells of the neocortex (Chang and Dyer, 1985; Aschner and Aschner, 1992; Koczyk, 1996; McCann et al., 1996; Nilsberth et al., 2002; Geloso et al., 2011; Kuramoto et al., 2011; Lattanzi et al., 2013).

In animal models TMT treatment induces behavioral alterations such as hyperactivity, hyperexcitability, aggression and cognitive deficits that include memory loss and learning impairment (Dyer et al., 1982a,b; Chang and Dyer, 1983; Balaban et al., 1988).

The molecular mechanisms that mediate TMT-induced toxicity have not yet been completely elucidated, although many hypotheses have been formulated (Patel et al., 1990; Pavlaković et al., 1995; Gunasekar et al., 2001; Geloso et al., 2002): the neurotoxicant action has nonetheless been shown to be mediated by intracellular Ca^{2+} concentration overload in cultured rat hippocampal neurons (Piacentini et al., 2008), in HeLa and neuroblastoma cells (Florea et al., 2005a,b) and also in spiral ganglion cells (Fechter and Liu, 1995). In this respect, it is noteworthy that rat hippocampal neurons expressing the Ca^{2+}-binding proteins calretinin and parvalbumin are selectively spared by the neurotoxicant (Geloso et al., 1996, 1997, 1998; Businaro et al., 2002; Gangitano et al., 2006), possibly through a calcium-buffering effect. Finally, we have previously demonstrated that lysosomal protease cathepsin D

*Corresponding author. Tel: +39-06-30155848; fax: +39-06-30155753.
E-mail address: fabrizio.michetti@rm.unicatt.it (F. Michetti).

Abbreviations: AQP4, Aquaporin 4; BBB, blood–brain barrier; FC, fold change; GFAP, glial acidic fibrillary protein; i.p., intraperitoneal; IgG, immunoglobulin G; MRI, magnetic resonance imaging; NDS, normal donkey serum; NeuN, neuronal nuclei; PB, phosphate buffer; PBS, phosphate-buffered saline; PFA, paraformaldehyde; PVDF, polyvinylidene fluoride; RECA-1, rat endothelial cell antigen-1; RT, room temperature; SDS–PAGE, sodium dodecyl sulfate–polyacrylamide gel electrophoresis; TBS-T, Tris–buffered saline–Tween; TMT, trimethyltin; VEGF, vascular endothelial growth factor; VEGFR-2, vascular endothelial growth factor receptor-2; VEGFR-2P, vascular endothelial growth factor receptor-2 phosphate.

http://dx.doi.org/10.1016/j.neuroscience.2014.05.047
0306-4522/© 2014 IBRO. Published by Elsevier Ltd. All rights reserved.

plays a crucial role in the TMT-induced hippocampal neurodegeneration process in a calcium-dependent manner (Ceccariglia et al., 2011).

TMT neurodegeneration is also accompanied by an increased expression of astrocytes and activation of microglial cells (Koczyk and Oderfeld-Nowak, 2000; Geloso et al., 2004; Reali et al., 2005; Röhl and Sievers, 2005; Little et al., 2012). There is also increasing evidence that astrocytic cells play a crucial role in neurological disorders and may be considered a potentially useful target to address brain injury (Steinhäuser and Seifert, 2002; Tian et al., 2005; Binder and Steinhäuser, 2006; Seifert et al., 2006).

Aquaporins (AQPs) are a family of plasma membrane water-channel proteins expressed in many tissues and cell types (Verkman, 2002, 2005). In particular, Aquaporin 4 (AQP4), the most studied member of this family, is expressed in the brain and is localized mainly in pericapillary astrocytic end-feet (Nielsen et al., 1997; Rash et al., 1998; Iacovetta et al., 2012). This pattern of distribution suggests an active role for AQP4 in the control of water flow into and out of the brain, although this protein has also been proposed to be involved in astrocyte migration and in the regulation of neuronal activity (e.g. synaptic plasticity) (Nagelhus et al., 2004; Tait et al., 2008; Iacovetta et al., 2012; Nagelhus and Ottersen, 2013; Scharfman and Binder, 2013). Essentially, AQP4 is regarded as a specific marker of vascular permeability and, in general, its deregulation is believed to be potentially associated with damage to the blood–brain barrier (BBB) and to play a role in brain edema (Vizuete et al., 1999; Ke et al., 2001; Nico et al., 2003; Warth et al., 2007; Nico and Ribatti, 2012). An altered expression of AQP4 has been studied in several, different diseases such as cerebral ischemia, brain traumatic injury, brain tumors, hydrocephalus and kainic acid-induced status epilecticus (Taniguchi et al., 2000; Saadoun et al., 2002; Nesic et al., 2006; Aghayev et al., 2012; Lee et al., 2012).

To date, the role of AQP4 protein in TMT neurotoxicity has not been studied, though a magnetic resonance imaging (MRI) investigation, in TMT-treated rats, evidenced dilation of lateral ventricles also suggesting alterations in blood–brain barrier permeability and brain edema (Andjus et al., 2009).

Vascular endothelial growth factor A (VEGF-A, abbreviated as VEGF) and its main receptor-2 (VEGFR-2) are known for their essential roles in blood vessel growth, neurogenesis and neuroprotection (Morin-Brureau et al., 2011; Mackenzie and Ruhrberg, 2012; Licht and Keshet, 2013). Most importantly, previous studies have shown that the VEGF/VEGFR-2 pathway can also increase vascular permeability, thereby disrupting the BBB, and promote inflammatory cell infiltration in the nervous system (Proescholdt et al., 1999; van Bruggen et al., 1999; Zhang et al., 2000; Kilic et al., 2006; Lafuente et al., 2006).

The present study aimed to investigate AQP4 expression, vascular leakage and VEGF/VEGFR-2 signaling pathway in the rat hippocampus and cortex during TMT-induced neurodegeneration, in order to explore possible molecular mechanisms involved in alterations to vascular permeability and brain edema occurring in this experimental model of neurodegeneration.

EXPERIMENTAL PROCEDURES

Animals and treatment

Experiments were performed using adult female Wistar rats (200–250 g body weight, age 2 months). Animals were housed in an air-conditioned environment with constant temperature (25 °C) and a standardized light/dark schedule, food and water being supplied *ad libitum*. The rats were treated with a single intraperitoneal (i.p.) injection of TMT (Sigma, St. Louis, MO, USA) dissolved in saline 0.9% NaCl at a dose of 8 mg/kg body weight in a volume of 1 ml/kg body weight. Control rats received the same volume of saline solution. The animals were anesthetized by i.p. injection with 2 mg/100 g body weight of diazepam (Biologici Italia Laboratories, Milano) followed by 4 mg/100 g body weight of ketamine (Intervet International, GmbH, Germany) and then sacrificed 7, 14, 21 or 35 days after treatment. All the animal protocols were approved by the Animal Experimentation Committee of Catholic University, Rome. In particular, animal experiments were performed in accordance with the European Communities Council Directive of 24 November 1986 (86/609/EEC). Every effort was made to minimize the number of animals used and their suffering.

AQP4 and glial acidic fibrillary protein (GFAP) real-time PCR analyses

AQP4 and GFAP expression levels were analyzed by quantitative real-time PCR (qPCR) in the rat hippocampus and cortex. Total RNA was isolated both from the entire hippocampus and from the cortex for each control and each 7-, 14-, 21- and 35-day TMT-treated animal (3 animals/group, sacrificed by decapitation after deep anesthesia) using Trizol reagent (Invitrogen, Carlsbad, CA, USA) and purified using the RNeasy MiniElute Cleanup Kit (Qiagen, Valencia, CA, USA), according to the manufacturer's instructions. An additional on-column DNAse incubation step was performed to allow the selective removal of genomic DNA during the isolation process. Thereafter, two-step reverse transcription and qPCR were carried out as previously described (Barba et al., 2012). The oligonucleotide primers were designed using Primer 3 software (http://bioinfo.ut.ee/primer3-0.4.0/), primer sequences are reported in Table 1.

Real-time PCR was performed in at least three independent experiments.

Western blotting analyses

For western blotting analyses, the entire hippocampus or cortex of control and TMT-treated (7, 14, 21, 35 days) rats (3 animals/group, sacrificed by decapitation after deep anesthesia) were dissected out and mechanically homogenized in radio immune precipitation assay

Table 1. List of primer sequences used in this study

Gene	Symbol	Sense	5′–3′ sequences
Actin-beta	ACTB	F	ATGGTGGGTATGGGTCAGAA
		R	GGTCATCTTTTCACGGTTGG
Aquaporin 4	AQP4	F	TGGCAGTTTTGTGTCTGTGG
		R	CGCCTTGGTTCTGTAGGTTC
Glial acidic fibrillary protein	GFAP	F	ACATCGAGATCGCCACCTAC
		R	ATGGTGATGCGGTTTTCTTC

(RIPA) buffer (50 mM Tris–HCL, pH 7.4, 150 mM NaCl, 1% Triton X-100, 0.1% SDS and 0.5% sodium deoxycholate) with a protease inhibitor cocktail (Sigma–Aldrich, St Louis, MO, USA) added just before use. Homogenized tissues were incubated on ice for 30 min and then centrifuged at 14,000 rpm for 30 min at 4 °C. The supernatants were collected and protein concentrations were determined using Lowry's method (Lowry et al., 1951).

Equal amounts of protein (40 μg/lane) from each sample were electrophoresed on 8–12% SDS–PAGE and western blotted at 100 V for 2 h to Hybond polyvinylidene fluoride (PVDF) membranes (Amersham Biosciences, Uppsala, Sweden). Bovine serum albumin (5% w/v) in Tris–buffered saline (50 mM Tris–HCL, pH 7.4, 150 mM NaCl, 0.1% Tween 20) (TBS-T) was used to block the membranes for 1 h at room temperature (RT). After washing with TBS-T the membranes were incubated overnight at 4 °C with appropriate primary antibody: goat anti-AQP4, or rabbit anti-VEGF, or mouse anti-VEGFR-2 (1:100, Santa Cruz Biotechnology, CA, USA), or rabbit anti-VEGFR-2P (phosphorylation sites on tyrosine 1054 and tyrosine 1059) (1:200, Abcam, Cambridge, UK) and mouse anti-β-actin (used to normalize each protein loading) (1:1000, Sigma–Aldrich). After extensive washing with TBS-T, PVDF membranes were incubated for 1 h at RT with adequate horseradish peroxidase-conjugated secondary antibody IgG (1:2000, Santa Cruz Biotechnology). After three washes, bands were visualized using Kodak BioMax light autoradiography. A GS-800 Calibrated Densitometer (Bio-Rad Hercules, CA, USA) was used to scan and store images of the immunoblotting. Densitometry was performed using Quantity One (Bio-Rad) software.

Western blotting analysis to determine the mature form (42 kDa) of VEGF factor was performed in non-reducing conditions.

For immunoglobulin G (IgG) analysis, the entire hippocampus or cortex of control and TMT-treated (14, 21, 35 days) rats (3 animals/group) was dissected out and processed as described above. After incubation with biotinylated goat anti rat-IgG secondary antibody (1:200, Vector Laboratories, Burlingame, CA, USA) and with an avidin–biotin peroxidase complex (ABC method, 1:500, Vector Laboratories), antibody reactivity was detected using 3,3′-diaminobenzidine tetrahydrochloride (Sigma–Aldrich) and 0.01% v/v hydrogen peroxide in phosphate-buffered saline (PBS). Monoclonal antibody against β-actin (1:20,000, Sigma–Aldrich) was used to normalize protein loading. The optical density of the heavy chain of IgG (~55 kDa) was analyzed by Bio-Rad Gel doc Bio-Rad Multi-analyst software.

All western blotting analyses were performed in at least three independent experiments.

Immunohistochemical localization of AQP4, VEGF and VEGFR-2

Under deep anesthesia the animals were perfused by a peristaltic pump through the aorta with 250 ml of saline solution, followed by 250 ml of 4% (w/v) paraformaldehyde (PFA) at a rate of 4–5 ml/min. About 30 min after perfusion brains were removed from the skull, post-fixed in 4% PFA overnight at 4 °C and transferred in phosphate buffer (PB) 0.1 M pH 7.4. Serial 40-μm-thick coronal sections were cut on a vibratome (Leica VT 1000S) and collected in a free-floating manner.

Tissue sections of control and 7-, 14-, 21- and 35-day TMT-treated animals (3 animals/group) were processed for triple and double immunofluorescence labeling. Non-specific binding sites were blocked with 5% normal donkey serum (NDS) in PBS 0.01 M pH 7.4 for 1 h at RT. One first series of sections was incubated with the following primary antibodies: goat anti-AQP4 (1:200, Santa Cruz Biotechnology), rabbit anti-vascular endothelial growth factor (VEGF) (1:100, Santa Cruz Biotechnology) and mouse anti-GFAP for astrocytes (1:500, Chemicon, Temecula, CA, USA) or mouse anti-Neu N antibody for neurons (1:500, Chemicon). A second series of slices was incubated with the following primary antibodies: mouse anti-VEGF receptor-2 (VEGFR-2 also named Flk-1, 1:100, Santa Cruz Biotechnology) and rabbit anti-VEGF (1:100, Santa Cruz Biotechnology). After incubation in primary antisera overnight at 4 °C, sections were rinsed three times with PBS and then exposed to the appropriate donkey secondary antibodies: Cy3 anti-goat for AQP4 (1:400, Jackson Immunoresearch Laboratories, West Grove, PA, USA), Alexa Fluor 647 (1:200, Jackson Immunoresearch Laboratories) and Cy2 (1:250, Jackson Immunoresearch Laboratories) anti-rabbit for VEGF, Alexa Fluor 488 anti-mouse for GFAP and neuronal nuclei (NeuN) (1:250, Jackson Immunoresearch Laboratories) and Cy3 anti-mouse for VEGFR-2 (1:400, Jackson Immunoresearch Laboratories), for 1 h at RT. After further washing, sections were mounted on glass slides, cover-slipped with gel-mount anti-fading mounting medium (Sigma–Aldrich), examined and photographed under a Zeiss LSM 510 confocal laser scanning microscopy system.

The specificity of the labeling was confirmed by incubation of sections with only the secondary antibodies, omitting the primary antisera. No immunoreactivity was observed under these conditions.

Five non-consecutive sections were immunostained from each animal/time point.

IgG immunofluorescence labeling

In order to investigate possible TMT-induced damage of the BBB, we assessed the degree of endogenous IgG leakage in the rat hippocampus and cerebral cortex using immunofluorescence labeling with fluorescein anti-rat IgG antibody. Because IgGs are not normally present in brain parenchyma (but are restricted to the inside of vessels), immunoreactivity of these molecules in brain parenchyma is regarded as a reliable indicator of BBB alteration (Rigau et al., 2007; Sun et al., 2012).

IgG immunofluorescence was investigated in the hippocampus and cortex of controls and 14-, 21- and 35-day TMT-treated rats (3 animals/group). The animals were perfused as described above.

Serial 30-μm-thick coronal sections were cut on a vibratome and processed for double label immunofluorescence.

After several rinses with PBS, tissue sections were blocked with 5% NDS in PBS for 1 h at RT, followed by incubation overnight at 4 °C with the primary antibodies against: mouse rat endothelial cell antigen-1 (RECA-1) (1:250, AbD Serotec, Kidlington, Oxford, UK), for some sections, and mouse anti-NeuN (1:500, Chemicon) for the others. After incubation in primary antisera, sections were rinsed with PBS, exposed to the appropriate secondary antibodies: donkey Cy3 anti-mouse (1:400, Jackson Immunoresearch Laboratories) for 1 h at RT and then incubated with rabbit fluorescein anti-rat IgG secondary antibody (1:250, Vector Laboratories) overnight at 4 °C. After further washing, sections were processed, observed and photographed as described above.

Background staining was not observed in negative control sections, when the primary antisera were omitted.

Five non-consecutive sections were immunostained from each animal/time point.

Statistical analysis

The real-time PCR results are expressed as fold changes (FC), calculated according to the ΔΔCt method, and presented as mean ± SEM. For statistical analyses, group differences were evaluated using a one-way analysis of variance [Analysis of Variance (ANOVA) Calculator-One-Way ANOVA from Summary Data-Software. Available from http://www.danielsoper.com/statcalc] and the Bonferroni post-hoc test, assuming the level of probability $^{*}P < 0.05$ as significant. For western blotting results, data are expressed as mean ± SEM. Statistical analyses were performed by a one-way ANOVA followed by Fisher's test, assuming the levels of probability $^{*}P < 0.05$ and $^{***}P < 0.001$ as significant.

RESULTS

AQP4 protein is over-expressed after TMT treatment and is localized in astrocytic cells

We analyzed AQP4 and GFAP gene expression at different intervals after TMT treatment (7, 14, 21 and 35 days). Real-time PCR analysis revealed a significant up-regulation ($P < 0.05$) of the AQP4 gene in the hippocampus, starting 14 days after treatment (FC = 4.1); this up-regulation remained significantly high at 21 (FC = 3.8) and 35 days (FC = 4.6) (Fig. 1A). The level of AQP4 in the cortex was also significantly up-regulated ($P < 0.05$) starting from 14 days after treatment (FC = 3.7), but decreased slightly after 21 (FC = 2.9) and 35 days (FC = 2.7) (Fig. 1B) while remaining statistically significant. GFAP gene expression showed significant up-regulation ($P < 0.05$) already 7 days after treatment in both the hippocampus (FC = 6.8) and the cortex (FC = 3.9). The GFAP expression level was higher 14 days after treatment in both the hippocampus (FC = 14.1) and the cortex (FC = 9.7). After 21 and 35 days of intoxication the GFAP gene expression decreased in both tissues but remained statistically significant (hippocampus at 21 and 35 days: FC = 13.2 and 11.6 respectively; cortex at 21 and 35 days: FC = 5.4 and 5 respectively) (Fig. 1C, D).

In order to analyze AQP4 protein expression, western blotting analysis was carried out 7, 14, 21 and 35 days after toxin administration. AQP4 protein was significantly over-expressed ($P < 0.001$) from 14 to 35 days in the hippocampus (Fig. 2A). Similarly, in the cortex we observed a significant albeit less marked increase ($P < 0.05$) at 14 days in AQP4 levels, which were further increased ($P < 0.001$) 21 and 35 days after treatment (Fig. 2B).

In order to visualize the distribution and cellular localization of the AQP4 immunoreactivity in the hippocampus and cortex of control and TMT-treated rats, immunofluorescence experiments using an antibody to AQP4 in combination with GFAP and NeuN markers, were performed.

In all hippocampal regions and in the cerebral cortex areas, we observed moderate AQP4 co-localization with GFAP-positive astrocytic cells 7 days after TMT intoxication (Fig. 3H). From 14 to 35 days after treatment, AQP4 immunolabeling in the activated astrocytes exhibited a diffuse, marked increase, in accordance with PCR and blotting data, in both the hippocampus (Fig. 3J, N, R) and cortex areas (Fig. 4J, N, R), where an intense and reactive astrocytosis was observed (Figs. 3 and 4I, M, Q). AQP4 immunoreactivity was localized in astrocyte end-feet surrounding blood vessels, as expected. We also observed that AQP4 immunolabeling was not completely co-localized with GFAP staining in either the hippocampus or the cortex at any of the time-points analyzed. This is in accordance with the observation of Simard and Nedergaard (2004) that many fine leaflet astrocytic processes are not labeled with anti-GFAP antibodies.

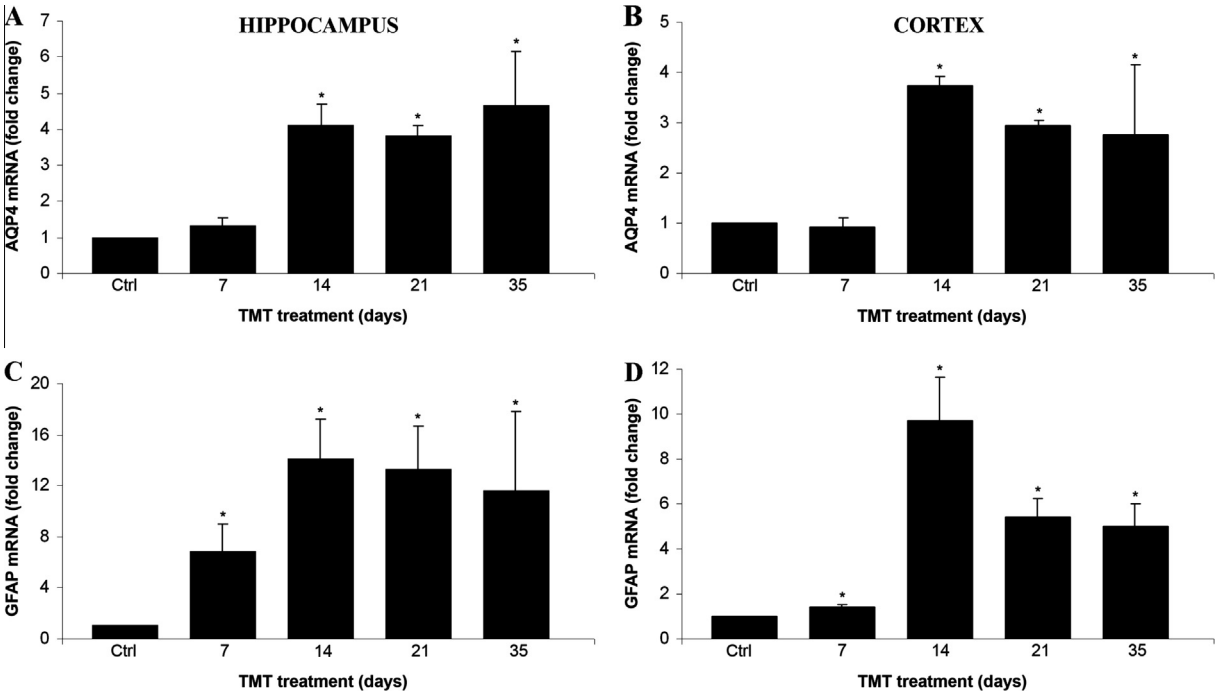

Fig. 1. Quantitative real-time PCR gene expression analysis of AQP4 and GFAP in rat hippocampus and frontal–parietal cortex after TMT treatment. (A–D) Graphic presentations of AQP4 and GFAP gene expression are shown. Values are expressed as fold changes, calculated according to the ΔΔCt method and presented as mean ± SEM for each time point tested (Ctrl, 7, 14, 21 and 35 days after TMT treatment, $n = 3$/group), $^{*}P < 0.05$ compared with controls, Bonferroni post-hoc test. Ctrl: control sample.

All the experiments performed on the control animals evidenced only weak AQP4 labeling (Figs. 3 and 4B) co-localized with GFAP (Figs. 3 and 4A).

AQP4 protein did not co-localize with NeuN-positive neuronal cells of either the hippocampus or the cortex at any time after TMT treatment (Fig. 7D, H).

IgG is extravasated after TMT treatment

In order to investigate the effects of TMT on BBB integrity, we first measured endogenous IgG levels by western blotting analysis in the hippocampus and cortex homogenates of control and toxin-treated (14, 21 and 35 days) rats. Protein levels increased significantly ($P < 0.05$) at 21 days in the hippocampus and decreased at 35 days, while remaining higher than in the controls (Fig. 2G). The levels of cortex IgG increased moderately at 21 and 35 days after toxin administration (Fig. 2H). No IgG increase (compared with control values) was observed 14 days after treatment in either the hippocampus or the cortex (data not shown).

We then evaluated extravasation of IgG by double label immunofluorescence experiments using an anti-rat IgG fluorescein antibody in combination with a vascular endothelium (RECA-1) or neuronal marker (NeuN), because of the importance of endothelial and neuronal components in the context of BBB alteration.

We observed partial immunolabeling of both IgG and RECA-1 in the CA1 hippocampal subfield (Fig. 5F) and in some cortical areas (Fig. 6F) 21 days after TMT treatment. In addition, at the same time after treatment (21 days), we found, in the CA3 and in some cortical regions, extra-vascular IgG staining (green staining) diffused in the paravasal parenchyma (Figs. 5K and 6H). It is also interesting to note that 35 days after toxicant administration the immunofluorescence images showed a selective accumulation of IgG in the cytoplasm of a few residual neurons scattered in the hippocampus (Fig. 5R). Similarly, at the same treatment time (35 days), some IgG-positive neurons were clearly visible in the cortex (Fig. 6O). Some neuronal cells were faintly IgG-stained, whereas others were strongly IgG-labeled. Notably, many damaged IgG-positive neurons lost their NeuN immunogenicity.

The IgG extravasation was not seen 14 days after TMT treatment. As expected, no IgG staining was observed in control samples (Figs. 5B, H, N and 6B, K).

TMT induces VEGF/VEGFR-2 pathway over-expression and VEGFR-2 activation in neuronal cells

To examine the possible implications of VEGF and VEGFR-2 in the event of BBB impairment during TMT intoxication, we analyzed the expression and cellular localization of these proteins in both the hippocampus and cortex of control and TMT-treated rats.

We first measured the levels of VEGF and VEGFR-2 by immunoblotting at 7, 14, 21, 35 days after TMT treatment. VEGF protein levels were significantly increased ($P < 0.001$) starting from 7 days in both the hippocampus and the cortex and remained persistently over-expressed at later treatment times (14, 21, 35 days) (Fig. 2C, D).

To confirm further the role of VEGF protein, we evaluated the expression levels of its receptor

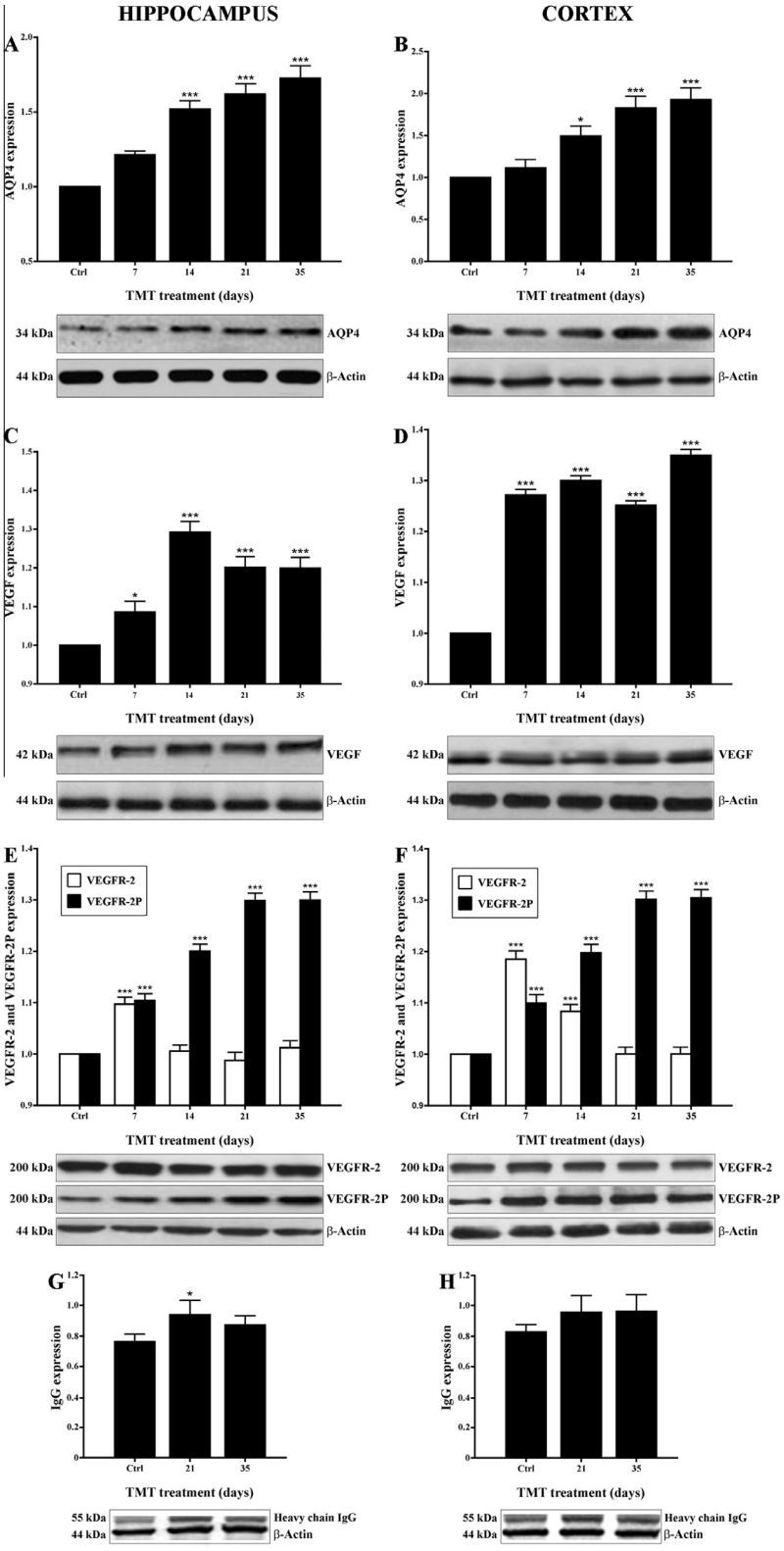

Fig. 2. TMT-induced increased expression of AQP4, VEGF, VEGFR-2, VEGFR-2P and IgG proteins in the rat hippocampus and frontal–parietal cortex. (A–H) Graphic presentations and western blotting images of AQP4, VEGF, VEGFR-2, VEGFR-2P proteins and IgG accumulation are shown. Values are presented as mean ± SEM for each group: the control rats (n = 3) and 7-, 14-, 21-, 35-day TMT-treated rats (n = 3/group), $^{*}P < 0.05$ and $^{***}P < 0.001$ compared with controls, Fisher's-test. Ctrl: control sample.

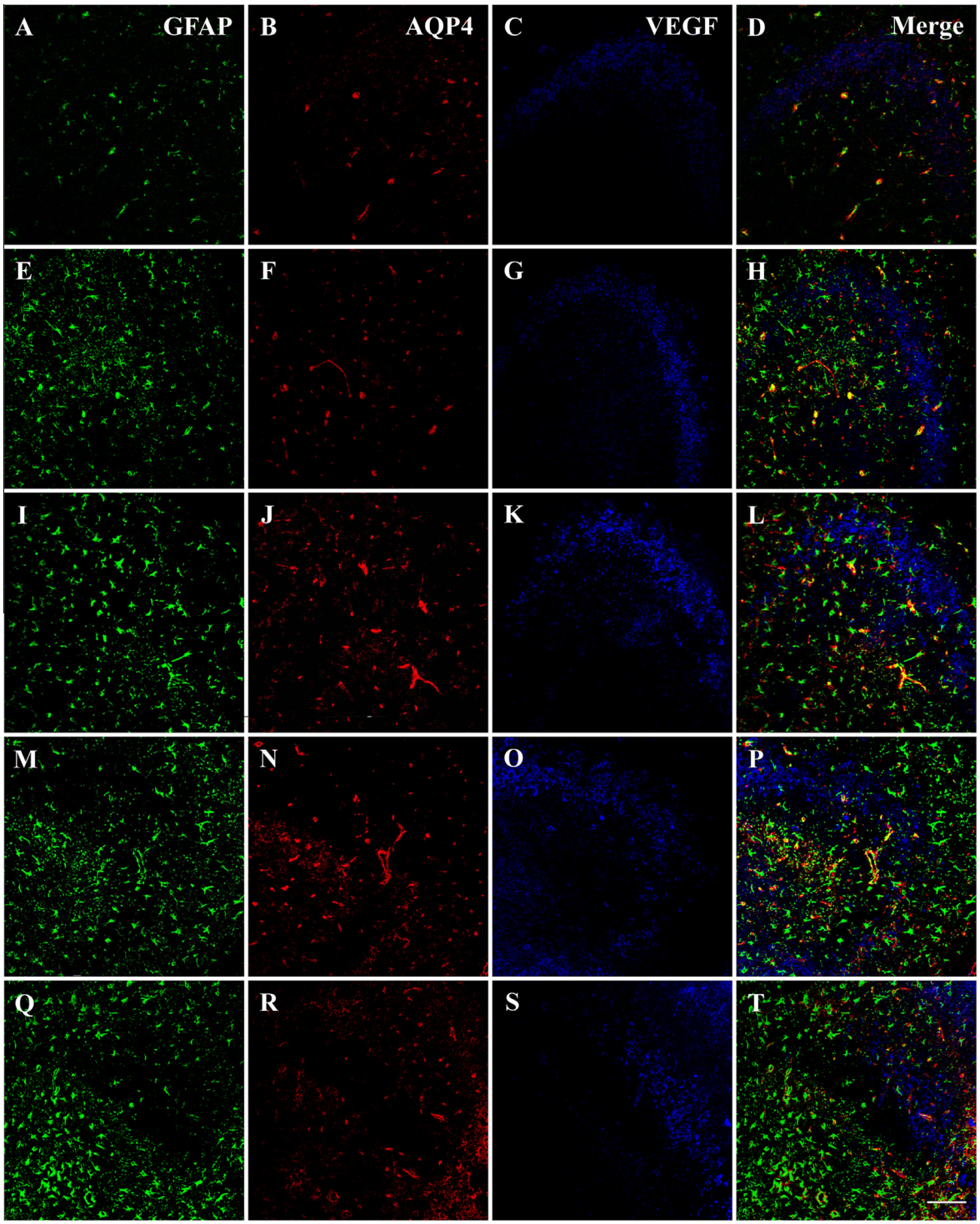

Fig. 3. Increased expression of AQP4 and VEGF in the rat hippocampus after TMT treatment. Sections of the CA3 region at different treatment times (7, 14, 21, 35 days) are triple-labeled for GFAP (green), AQP4 (red), VEGF (blue) and GFAP/AQP4/VEGF (merge). Control sections (A–D). After 7 days of toxicant administration AQP4 immunoreactivity (F) is faintly observed in GFAP-positive cells (E) and VEGF staining (G) is more pronounced compared with controls. At 14, 21 and 35 days after treatment a marked increase in both AQP4 immunoreactivity (J, N, R) in GFAP-labeled astrocytes (I, M, Q) and VEGF staining (K, O, S) is observed. Note the gradual increase in the number of GFAP-positive cells in TMT-treated rats (7, 14, 21, 35 days). Scale bar = 100 μm. Ctrl: control sample, d: days. (For interpretation of the references to color in this figure legend, the reader is referred to the web version of this article.)

VEGFR-2. The receptor expression was transiently and significantly increased ($P < 0.001$) at 7 days after TMT treatment in the hippocampus and at 7–14 days in the cortex, then gradually decreased to control values at later treatment times in both analyzed areas (Fig. 2E, F).

In addition, we measured a characteristic feature of VEGFR-2 activation: the trans-autophosphorylation of

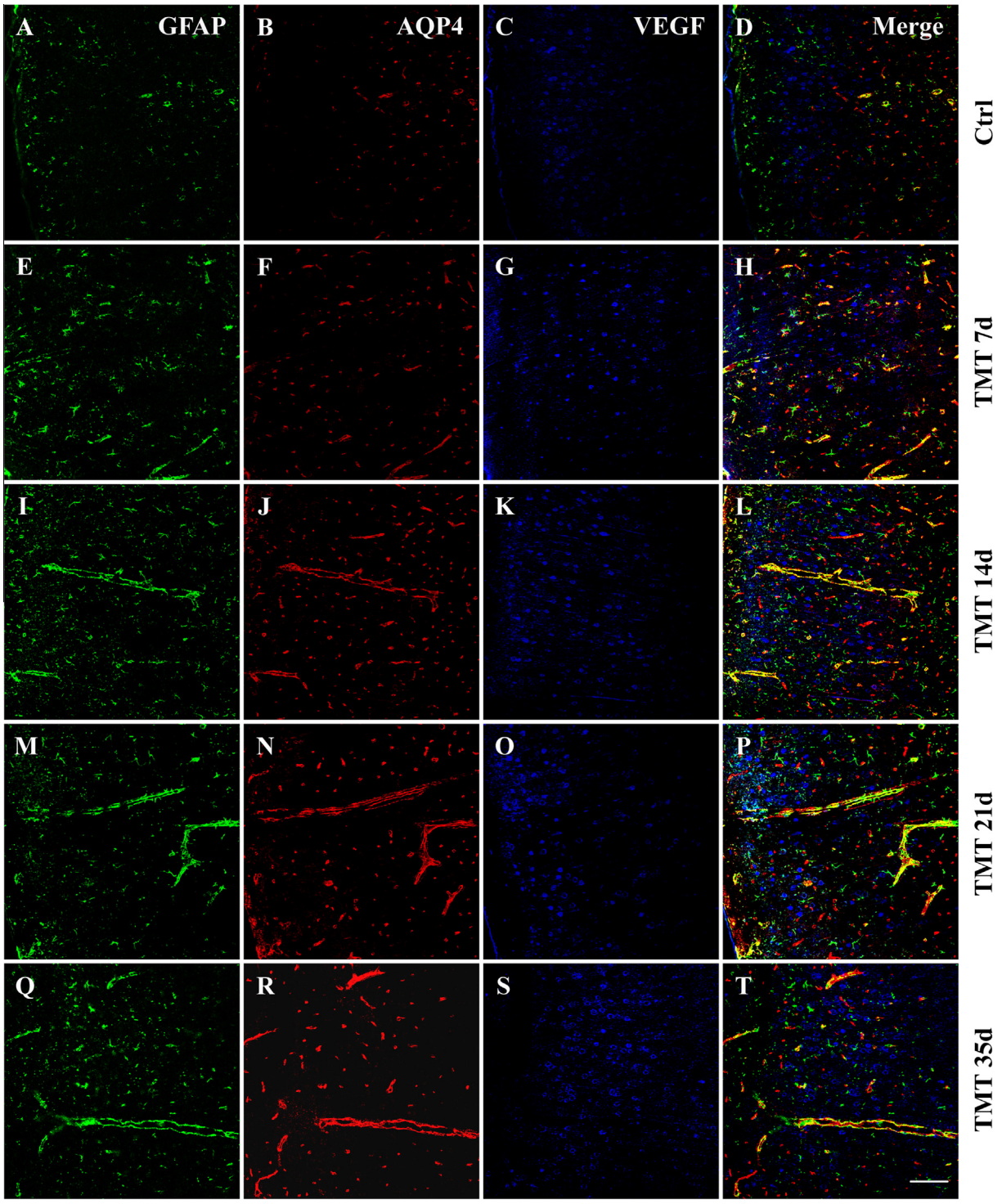

Fig. 4. Increased expression of AQP4 and VEGF in the rat cortex after TMT treatment. Sections of the frontal–parietal cortex at different treatment times (7, 14, 21, 35 days) are triple-labeled for GFAP (green), AQP4 (red), VEGF (blue) and GFAP/AQP4/VEGF (merge). Control sections (A–D). After 7 days of toxicant administration AQP4 immunoreactivity (F) is faintly observed in GFAP-positive cells (E) and VEGF staining (G) is more pronounced compared with controls. At 14, 21 and 35 days after treatment a marked and notable increase in both AQP4 immunoreactivity (J, N, R) in GFAP-labeled astrocytes (I, M, Q) and VEGF staining (K, O, S) is observed. Note the gradual increase in the number of GFAP-positive cells in TMT-treated rats (7, 14, 21, 35 days). Scale bar = 100 μm. Ctrl: control sample, d: days. (For interpretation of the references to colour in this figure legend, the reader is referred to the web version of this article.)

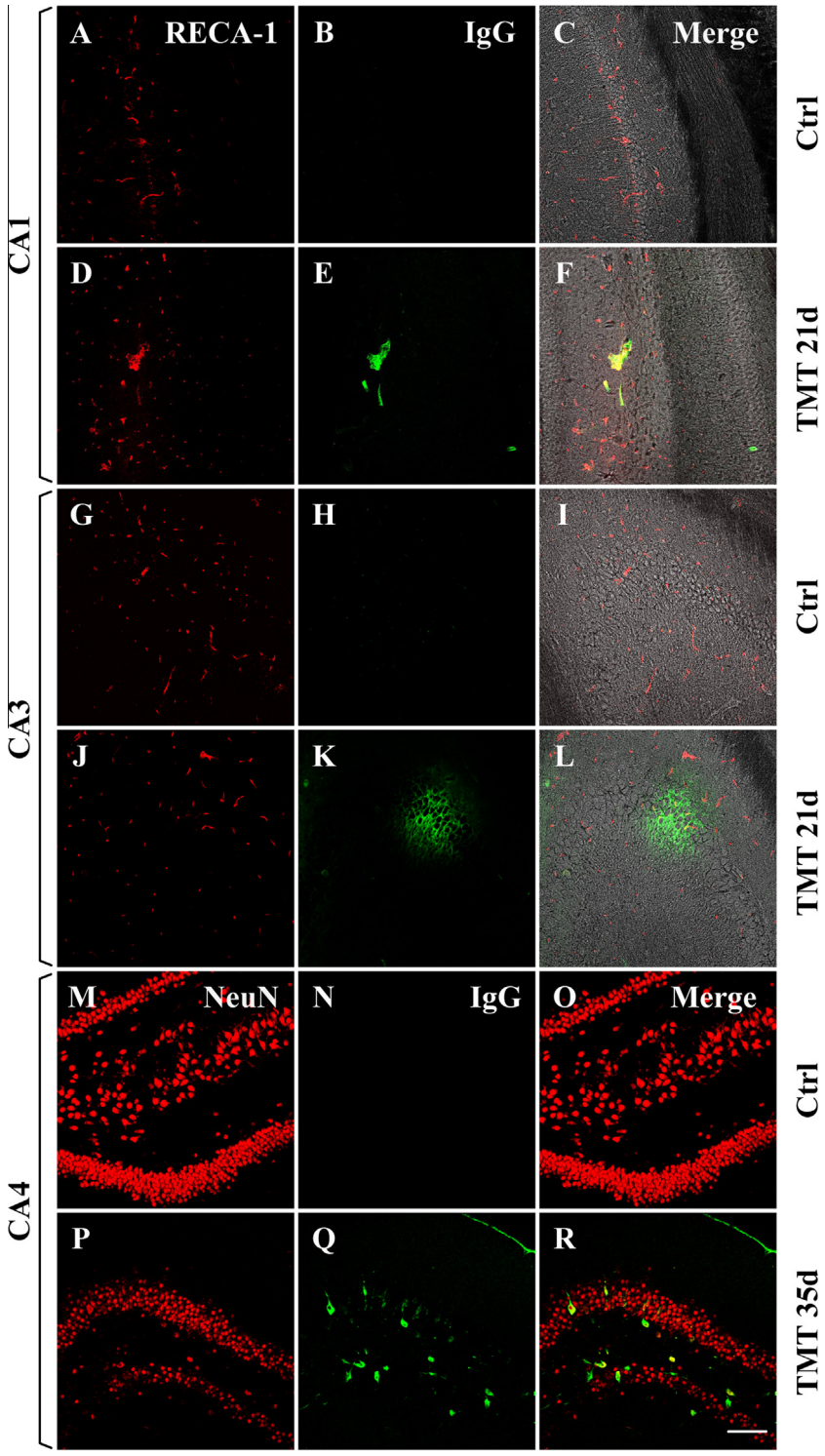

Fig. 5. Immunohistochemical localization of extravasated IgG in the rat hippocampus after TMT treatment. Double label immunofluorescence for endothelial cells (RECA-1, red, A, D, G, J) or neuronal cells (NeuN, red, M, P), IgG (green) and RECA-1/IgG or NeuN/IgG (merge) in control and TMT-treated rats (21, 35 days) is observed. IgG immunoreactivity is shown in CA1 (E) and CA3 (K) areas at 21 days and in CA4 area (Q) at 35 days after treatment. The merged images demonstrate co-localization of RECA-1/IgG (F), IgG extravasation in paravasal parenchyma (L) at 21 days of treatment and co-localization of NeuN/IgG (R) at 35 days. C, F, I, L merged images are overlapped with differential interference contrast images. No IgG staining is observed in control sections of CA1 (B), CA3 (H) and CA4 (N) fields. Scale bar = 100 μm. Ctrl: control sample, d: days. (For interpretation of the references to colour in this figure legend, the reader is referred to the web version of this article.)

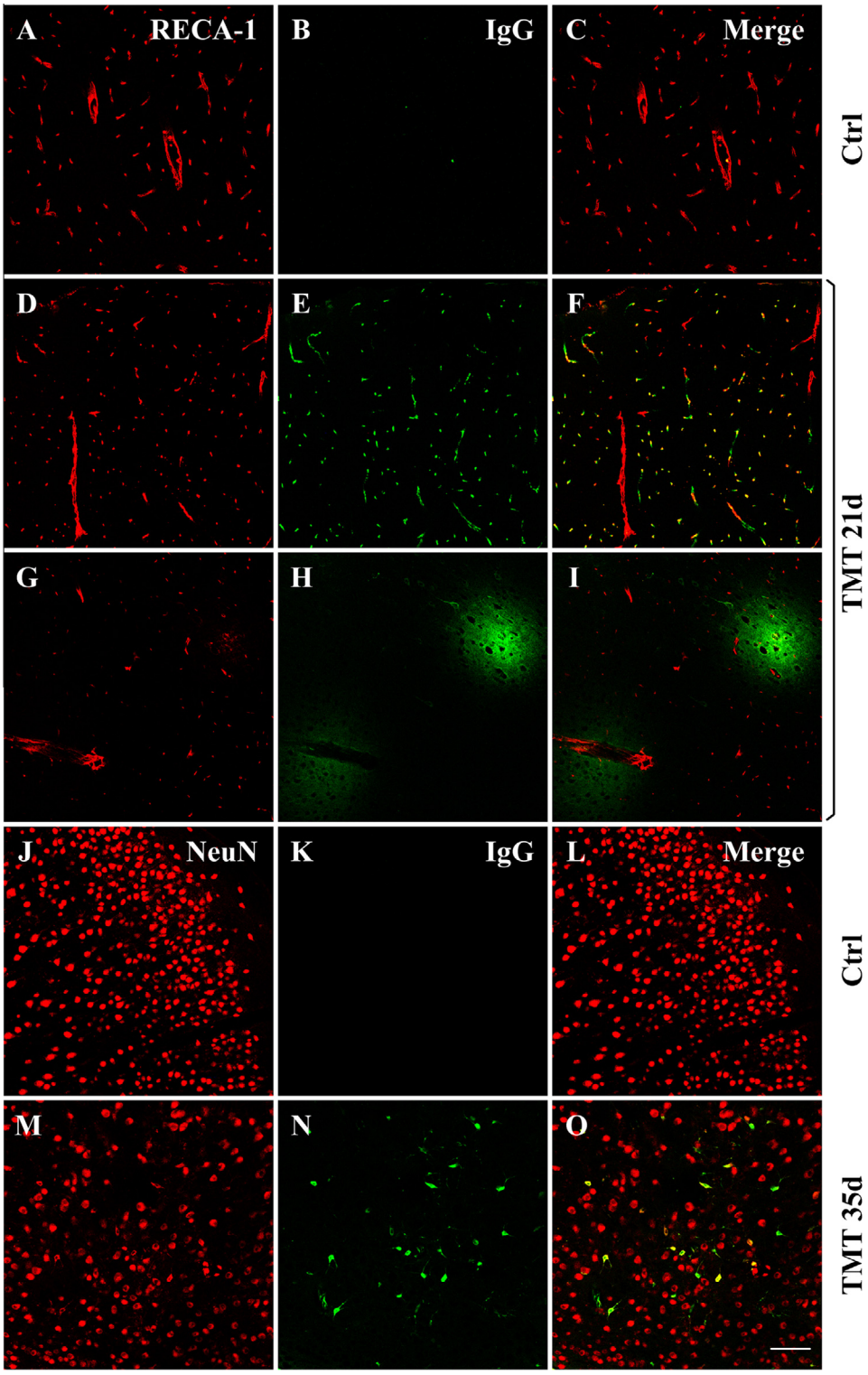

Fig. 6. Immunohistochemical localization of extravasated IgG in the rat frontal–parietal cortex after TMT treatment. Double label immunofluorescence for endothelial cells (RECA-1, red, A, D, G) or neuronal cells (NeuN, red, J, M), IgG (green), and RECA-1/IgG or NeuN/IgG (merge) in control and TMT-treated rats (21, 35 days) is observed. IgG immunoreactivity is shown in images (E, H) at 21 days and in image (N) at 35 days of treatment. The merged images show co-localization RECA-1/IgG (F), IgG extravasation in paravasal parenchyma (I) at 21 days of treatment and co-localization of NeuN/IgG (O) at 35 days. No IgG staining is observed in control sections (B, K). Scale bar = 100 μm. Ctrl: control sample, d: days. (For interpretation of the references to colour in this figure legend, the reader is referred to the web version of this article.)

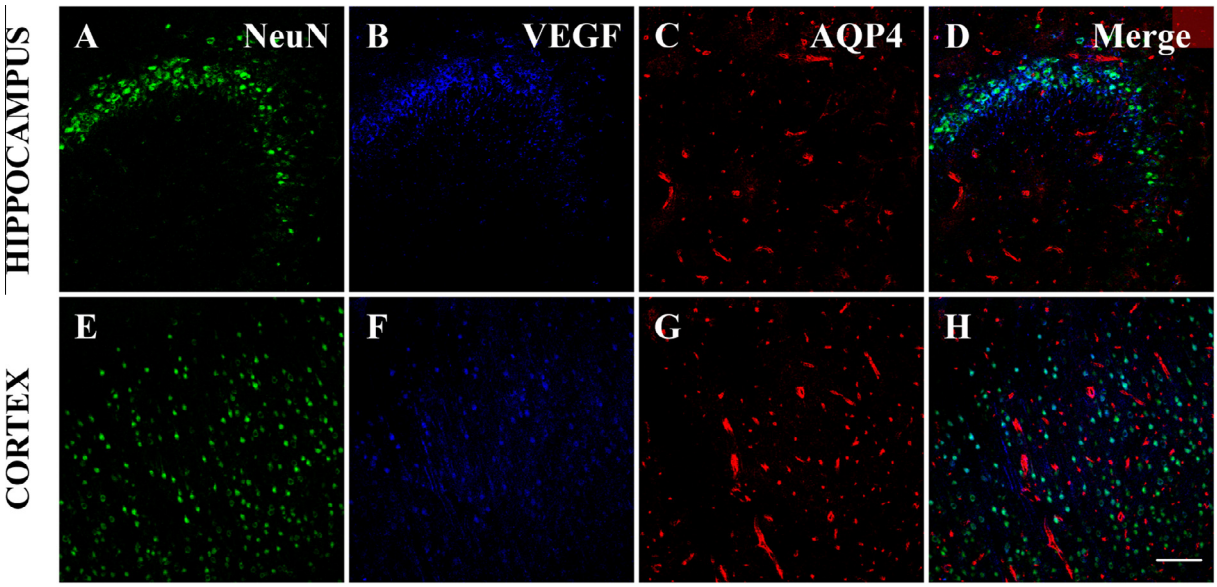

Fig. 7. Immunocytochemical characterization of cell types expressing VEGF and AQP4 in the rat hippocampus and cortex. Triple immunofluorescence labeling for NeuN (green, A, E), VEGF (blue, B, F), AQP4 (red, C, G) and NeuN/VEGF/AQP4 (merge, D, H) is shown in sections taken from CA3 hippocampal region and frontal–parietal cortex of TMT-treated rats (14 days). The merged images show that VEGF is co-localized with NeuN-positive neuronal cells and AQP4 protein is not expressed in neuronal cells. Scale bar = 100 μm. (For interpretation of the references to colour in this figure legend, the reader is referred to the web version of this article.)

tyrosine residues Y1054/Y1059 in the cytoplasmatic domain following receptor activation by VEGF (Dougher and Terman, 1999). The immunoblotting analysis showed that the levels of phospho Y1054/Y1059 (i.e. VEGFR-2P) were significantly increased ($P < 0.001$) on day 7 and this increase persisted to 35 days in both the hippocampus (Fig. 2E) and the cortex (Fig. 2F).

Finally, we also performed a series of immunolabeling experiments to identify the cell type(s) expressing VEGF and VEGFR-2 factors during TMT treatment. VEGF immunoreactivity was localized only in neuronal cells (by VEGF/NeuN co-localization), mainly in the soma of hippocampal (Fig. 7D) and cortical neurons (Fig. 7H), and VEGFR-2 staining co-localized with the VEGF-positive neuronal cells in both the hippocampus (Fig. 8F) and the cortex (Fig. 8L).

DISCUSSION

The present results show that AQP4 is up-regulated in both the rat hippocampus and the cortex during neurodegenerative processes triggered by TMT.

AQP4 water channels are known to be primarily expressed in astrocytes surrounding blood vessels in the brain (Vizuete et al., 1999; Ke et al., 2001; Papadopoulos and Verkman, 2007; Saadoun and Papadopoulos, 2010; Iacovetta et al., 2012). Our data show AQP4 immunoreactivity to be increased and diffuse in perivascular astrocytes between 14 and 35 days after treatment in all hippocampal (Fig. 3J, N, R) and (frontal–parietal) cerebral cortex areas (Fig. 4J, N, R). RT-PCR and western blotting analyses also show significant up-regulation respectively of AQP4 mRNA (Fig. 1A, B) and protein expression (Fig. 2A, B) in all the areas analyzed, at the same time points (14–35 days) after toxicant treatment. Both in the hippocampus and in the cortex the over-expression of AQP4 appears to be related to TMT-induced reactive astrocytosis, as evidenced by immunofluorescence (Figs. 3 and 4E, I, M, Q). Activation of astrocytes in response to TMT, which is a well-known phenomenon, is also confirmed by the increased mRNA level of GFAP, which is a recognized hallmark of reactive astrocytes (Koczyk and Oderfeld-Nowak, 2000; Jahnke et al., 2001; Pekny and Nilsson, 2005). In addition, AQP4 and GFAP gene expression analysis during toxicant treatment revealed a direct correlation between AQP4 and GFAP mRNA up-regulation (between 14 and 35 days after treatment) (Fig. 1), the increase in GFAP mRNA being higher and earlier (7 days) than that in AQP4 mRNA. This might suggest that the delayed induction of AQP4 does not participate in the initiation of astrogliosis and the up-regulation of protein is linked to an increased glial reaction rather than to an increase in the protein in each individual astrocyte. It is possible that AQP4 participates in an apparent dilation of lateral ventricles as suggested by Andjus and collaborators (2009). It is also noteworthy, in this respect, that TMT treatment also reduces the wet weight of the hippocampus in a time- and dose-dependent fashion (Brock and O'Callaghan, 1987). The possibility that this reduction in hippocampal weight would participate to the appearance of dilated ventricles should also be taken into account, although the TMT-induced effects do not produce an extended and massive brain atrophy, being essentially restricted to the hippocampus.

At present it is unclear which signaling pathway may lead to AQP4 expression changes in astrocytes following TMT neurodegeneration. Many conditions have been reported to induce modifications in the expression of AQP4. In this respect, it has been

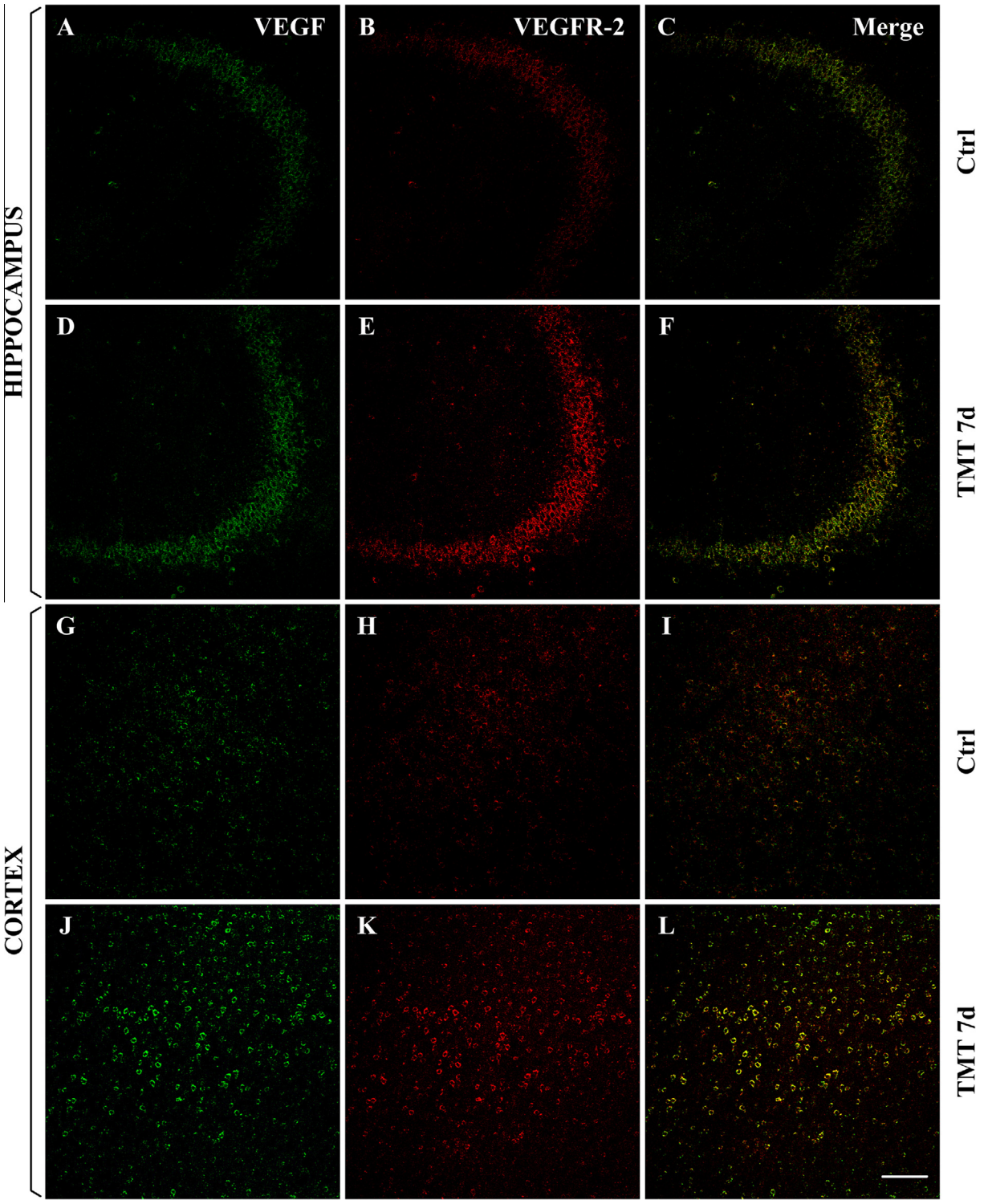

Fig. 8. VEGFR-2 is expressed on VEGF-positive neurons of the rat hippocampus and cortex in control and TMT-treated rats. Double immunofluorescence labeling for VEGF (green), VEGFR-2 (red) and VEGF/VEGFR-2 (merge) of the CA3 hippocampal region and frontal–parietal cortex of control (A–C and G–I) and TMT-treated rats (7 days, D–F and J–L). Note the VEGF and VEGFR-2 increased expression 7 days after treatment. Scale bar = 100 μm. Ctrl: control sample, d: days. (For interpretation of the references to colour in this figure legend, the reader is referred to the web version of this article.)

reported that exposure of the brain to hypo-osmotic shock increases AQP4 protein levels (Vajda et al., 2000), and that endothelin-1, which increases after stroke, induces AQP4 expression and edema (Lo et al., 2005). Interestingly, Arima et al. (2003) showed that hyperosmotic stress induced by mannitol increased the expression of AQP4 in cultured rat astrocytes, suggesting that oxidative stress mechanisms are involved in AQP4 expression regulation. It is interesting, in this respect, that several authors have demonstrated that

TMT-mediated neurotoxicity is associated with an increase in oxidative stress in both animal and cell models (Shin et al., 2005; Qu et al., 2011; Kaur and Nehru, 2013).

Considering the potential roles of AQP4 in brain edema (Papadopoulos and Verkman, 2007; Saadoun and Papadopoulos, 2010), we also evaluated the level of BBB integrity by immunostaining extravasated endogenous rat IgG, which is regarded as a marker of BBB injury (Rigau et al., 2007; Sun et al., 2012), in both the rat hippocampus and cortex, 21–35 days following TMT treatment. The IgG levels increased significantly 21 days after treatment in the hippocampus (Fig. 2G), as already observed in conditions of BBB impairment (Chen et al., 2008; Jalal et al., 2012; Sun et al., 2012). In fact, the extravasation of IgG in cases of BBB impairment has been described in several diseases of the central nervous system (Ryu and McLarnon, 2009; Ndode-Ekane et al., 2010; Michalak et al., 2012, 2013). In our study, we found moderate IgG immunolabeling in endothelial capillary cells and/or in the brain parenchyma outside blood vessels, as evidenced by double-labeling studies using the endothelial marker RECA-1 (Figs. 5F, L and 6F, I). In the areas investigated, some neuronal cells also appeared to be IgG-labeled (Figs. 5R and 6O). Based on the assumption that neurons double-labeled by anti-NeuN and anti-IgG antibodies have ingested IgG, this finding could be interpreted as TMT-induced cellular damage, as has been shown in ischemic brain tissue (Michalski et al., 2010). In addition, we observed IgG-positive neurons (35 days after intoxication) that displayed marked evidence of degeneration and loss of NeuN staining.

Our findings on IgG leakage are not consistent with those obtained by a previous study (Little et al., 2002), which found that exposure of rats to TMT did not result in extravascular immunostaining of IgG in the hippocampus 21 days after intoxication. This discrepancy could reasonably be due to different IgG staining methods used and to their different sensitivity (avidin/biotin complex system versus immunofluorescence used in the present study). However, our data on the quantification of IgG levels are in agreement with those of the same Authors, who also found a significant increase in IgG 21 days after treatment. In any case, it is noteworthy that we observed both AQP4 increase and IgG leakage in the same areas (hippocampus and frontal/parietal cortex) in which edema has been observed using MRI investigation during TMT-induced neurodegeneration (Andjus et al., 2009).

In addition, we analyzed cellular localization and expression of VEGF growth factor and its VEGFR-2 receptor, thought to be involved in alterations in vascular permeability, in both the hippocampus and the cortex. We observed an over-expression of VEGF (Fig. 2C, D) and its VEGFR-2 receptor, as well as receptor activation by its phosphorylation (VEGFR-2P) (Fig. 2E, F), in both hippocampal (Figs. 7D and 8F) and cortical neurons (Figs. 7H and 8L).

In the present study, VEGF and VEGFR-2 expression was restricted to neurons both of the hippocampus and cortex in control and TMT-treated rats, while in some neurological disorders (Carmeliet and Storkebaum, 2002), and in seizure disorders (Croll et al., 2004) VEGF and VEGFR-2 have been reported to be expressed both in neurons and glial cells. This finding suggests that glial cells, differently from neurons, are not directly involved in TMT-induced VEGF/VEGFR-2 signaling pathway. This finding is consistent with data observed during ischemic preconditioning (Lee et al., 2009), while the biological meaning of the exclusive involvement of neurons in VEGF/VEGFR-2 signaling pathway regulation in these brain injury models deserves further investigation.

Interestingly, an involvement of the neuronal VEGF/VEGFR-2 system in BBB integrity has been suggested in several neuroinflammatory pathologies such as experimental autoimmune encephalomyelitis, Alzheimer's disease and kainate-induced epilepsy (Ballabh et al., 2004; Zlokovic, 2008; Argaw et al., 2009; Morin-Brureau et al., 2011). It is also interesting, in this respect, that VEGFR-2 activation precedes IgG extravasation, as well as continuing during the latter phenomenon. These findings might hint at a pivotal role for the VEGF/VEGFR-2 system in initiating TMT-induced BBB leakage in the analyzed areas. This is in accordance with a previous study (Kilic et al., 2006) demonstrating that these factors are related to BBB permeability after focal cerebral ischemia.

Taken together, our data show that the expression of AQP4 protein during the development of the TMT-derived degenerative process, as analyzed by western blotting and immunofluorescence, is correlated with AQP4 mRNA findings; AQP4 expression also appears to be correlated with reactive astrocytosis, as evidenced by GFAP immunofluorescence and mRNA analysis. On the basis of these findings, the early and long-lasting induction of AQP4 may suggest a relevant role of this water channel in the formation/clearance of brain edema in the TMT neurodegeneration model.

Finally, these observations offer useful information that may better elucidate the critical role of this water-channel protein, which is currently regarded as a useful marker in neurological disorders such as brain edema, seizure and brain tumors (Papadopoulos et al., 2004; Binder and Steinhäuser, 2006; Papadopoulos and Verkman, 2007) and also as an important tool to identify new therapeutic approaches in these disorders.

CONCLUSIONS

We show AQP4 up-regulation and over-expression in perivascular astrocytes of the rat hippocampus and cortex, suggesting the possible involvement of this water channel protein in brain edema, as outlined by previous MRI investigations during TMT-induced neurodegeneration. We also show IgG leakage into the hippocampal and cortical paravasal parenchyma, as well as enhanced neuronal VEGF/VEGFR-2 production and VEGFR-2 activation (VEGFR-2P), both phenomena being regarded as being related to the increase in vascular leakage in a series of neurological diseases.

Acknowledgments—This work was supported by funds from Catholic University, Rome to C.G. and F.M. We would also like to thank Roberto Passalacqua, Klein Baltazar Del Carmen and Enrico Guadagni for their skilful technical support. We want also

to especially thank Prof. Pavle Andjus (University of Belgrade) for useful discussions.

REFERENCES

Aghayev K, Bal E, Rahimli T, Mut M, Balci S, Vrionis F, Akalan N (2012) Aquaporin-4 expression is not elevated in mild hydrocephalus. Acta Neurochir (Wien) 154:753–759.

Andjus PR, Bataveljić D, Vanhoutte G, Mitrecic D, Pizzolante F, Djogo N, Nicaise C, Gankam Kengne F, Gangitano C, Michetti F, Linden A, Pochet R, Bacić G (2009) In vivo morphological changes in animal models of amyotrophic lateral sclerosis and Alzheimer's-like disease: MRI approach. Anat Rec (Hoboken) 292:1882–1892.

Argaw AT, Gurfein BT, Zhang Y, Zameer A, John GR (2009) VEGF-mediated disruption of endothelial CLN-5 promotes blood–brain barrier breakdown. Proc Natl Acad Sci U S A 106:1977–1982.

Arima H, Yamamoto N, Sobue K, Umenishi F, Tada T, Katsuya H, Asai K (2003) Hyperosmolar mannitol simulates expression of aquaporins 4 and 9 through a p38 mitogen-activated protein kinase-dependent pathway in rat astrocytes. J Biol Chem 278:44525–44534.

Aschner M, Aschner JL (1992) Cellular and molecular effects of trimethyltin and triethyltin: relevance to organotin neurotoxicity. Neurosci Biobehav Rev 16:427–435.

Balaban CD, O'Callaghan JP, Billingsley ML (1988) Trimethyltin-induced neuronal damage in the rat brain: comparative studies using silver degeneration stains, immunocytochemistry and immunoassay for neurotypic and gliotypic proteins. Neuroscience 26:337–361.

Ballabh P, Braun A, Nedergaard M (2004) The blood–brain barrier: an overview: structure, regulation, and clinical implications. Neurobiol Dis 16:1–13.

Barba M, Pirozzi F, Saulnier N, Vitali T, Natale MT, Logroscino G, Robbins PD, Gambotto A, Neri G, Michetti F, Pola E, Lattanzi W (2012) Lim mineralization protein 3 induces the osteogenic differentiation of human amniotic fluid stromal cells through Kruppel-like factor-4 downregulation and further bone-specific gene expression. J Biomed Biotechnol 2012:813894.

Binder DK, Steinhäuser C (2006) Functional changes in astroglial cells in epilepsy. Glia 54:358–368.

Brock TO, O'Callaghan JP (1987) Quantitative changes in the synaptic vesicle proteins synapsin I and p38 and the astrocyte-specific protein glial fibrillary acidic protein are associated with chemical-induced injury to the rat central nervous system. J Neurosci 7:931–942.

Businaro R, Corvino V, Concetta Geloso M, De Santis E, Fumagalli L, Michetti F (2002) De novo expression of calretinin in trimethyltin induced degeneration of developing rat hippocampus. Brain Res Mol Brain Res 98:141–144.

Carmeliet P, Storkebaum E (2002) Vascular and neuronal effects of VEGF in the nervous system: implications for neurological disorders. Semin Cell Dev Biol 13:39–53.

Ceccariglia S, D'Altocolle A, Del Fa' A, Pizzolante F, Caccia E, Michetti F, Gangitano C (2011) Cathepsin D plays a crucial role in the trimethyltin-induced hippocampal neurodegeneration process. Neuroscience 174:160–170.

Chang LW, Dyer RS (1983) A time-course study of trimethyltin induced neuropathology in rats. Neurobehav Toxicol Teratol 5:443–459.

Chang LW, Dyer RS (1985) Septotemporal gradients of trimethyltin induced hippocampal lesions. Neurobehav Toxicol Teratol 7:43–49.

Chen X, Gawryluk JW, Wagener JF, Ghribi O, Geiger JD (2008) Caffeine blocks disruption of blood brain barrier in a rabbit model of Alzheimer's disease. J Neuroinflammation 5:12.

Croll SD, Goodman JH, Scharfman HE (2004) Vascular endothelial growth factor (VEGF) in seizures: a double-edged sword. Adv Exp Med Biol 548:57–68.

Dougher M, Terman BI (1999) Autophosphorylation of KDR in the kinase domain is required for maximal VEGF-stimulated kinase activity and receptor internalization. Oncogene 18:1619–1627.

Dyer RS, Walsh TJ, Wonderlin WF, Bercegeay M (1982a) The trimethyltin syndrome in rats. Neurobehav Toxicol Teratol 4:127–133.

Dyer RS, Wonderlin WF, Walsh TJ (1982b) Increased seizure susceptibility following trimethyltin administration in rats. Neurobehav Toxicol Teratol 4:203–208.

Fechter LD, Liu Y (1995) Elevation of intracellular calcium levels in spiral ganglion cells by trimethyltin. Hear Res 91:101–109.

Florea AM, Dopp E, Büsselberg D (2005a) Elevated Ca2 + (i) transients induced by trimethyltin chloride in HeLa cells: types and levels of response. Cell Calcium 37:251–258.

Florea AM, Splettstoesser F, Dopp E, Rettenmeier AW, Büsselberg D (2005b) Modulation of intracellular calcium homeostasis by trimethyltin chloride in human tumour cells: neuroblastoma SY5Y and cervix adenocarcinoma HeLa S3. Toxicology 216:1–8.

Gangitano C, Falasca C, Del Fa' A, Corvino V, Ceccariglia S, Zelano G, Geloso MC, Monego G, Michetti F (2006) Hippocampal calretinin-containing neurons cultured *in vitro* are resistant to trimethyltin induced neurodegeneration. Calcium Binding Proteins 1–2:120–124.

Geloso MC, Vinesi P, Michetti F (1996) Parvalbumin-immunoreactive neurons are not affected by trimethyltin-induced neurodegeneration in the rat hippocampus. Exp Neurol 139:269–277.

Geloso MC, Vinesi P, Michetti F (1997) Calretinin-containing neurons in trimethyltin-induced neurodegeneration in the rat hippocampus: an immunocytochemical study. Exp Neurol 146:67–73.

Geloso MC, Vinesi P, Michetti F (1998) Neuronal subpopulations of developing rat hippocampus containing different calcium-binding proteins behave distinctively in trimethyltin-induced neurodegeneration. Exp Neurol 154:645–653.

Geloso MC, Vercelli A, Corvino V, Repici M, Boca M, Haglid K, Zelano G, Michetti F (2002) Cyclooxygenase-2 and caspase 3 expression in trimethyltin-induced apoptosis in the mouse hippocampus. Exp Neurol 175:152–160.

Geloso MC, Corvino V, Cavallo V, Toesca A, Guadagni E, Passalacqua R (2004) Expression of astrocytic nestin in the rat hippocampus during trimethyltin-induced neurodegeneration. Neurosci Lett 357:103–106.

Geloso MC, Corvino V, Michetti F (2011) Trimethyltin-induced hippocampal degeneration as a tool to investigate neurodegenerative processes. Neurochem Int 58:729–738.

Gunasekar P, Li L, Prabhakaran K, Eybl V, Borowitz JL, Isom GE (2001) Mechanisms of the apoptotic and necrotic actions of trimethyltin in cerebellar granule cells. Toxicol Sci 64:83–89.

Iacovetta C, Rudloff E, Kirby R (2012) The role of aquaporin 4 in the brain. Vet Clin Pathol 41:32–44.

Jahnke GD, Brunssen S, Maier WE, Harry GJ (2001) Neurotoxicant-induced elevation of adrenomedullin expression in hippocampus and glia cultures. J Neurosci Res 66:464–474.

Jalal FY, Yang Y, Thompson J, Lopez AC, Rosenberg GA (2012) Myelin loss associated with neuroinflammation in hypertensive rats. Stroke 43:1115–1122.

Kaur S, Nehru B (2013) Alteration in glutathione homeostasis and oxidative stress during the sequelae of trimethyltin syndrome in rat brain. Biol Trace Elem Res 153:299–308.

Ke C, Poon WS, Ng HK, Pang JC, Chan Y (2001) Heterogeneous responses of aquaporin-4 in oedema formation in a replicated severe traumatic brain injury model in rats. Neurosci Lett 301:21–24.

Kilic E, Kilic U, Wang Y, Bassetti CL, Marti HH, Hermann DM (2006) The phosphatidylinositol-3 kinase/Akt pathway mediates VEGF's neuroprotective activity and induces blood brain barrier permeability after focal cerebral ischemia. FASEB J 20:1185–1187.

Koczyk D (1996) How does trimethyltin affect the brain: facts and hypotheses. Acta Neurobiol Exp (Wars) 56:587–596.
Koczyk D, Oderfeld-Nowak B (2000) Long-term microglial and astroglial activation in the hippocampus of trimethyltin-intoxicated rat: stimulation of NGF and TrkA immunoreactivities in astroglia but not in microglia. Int J Dev Neurosci 18:591–606.
Kuramoto N, Seko K, Sugiyama C, Shuto M, Ogita K (2011) Trimethyltin initially activates the caspase 8/caspase 3 pathway for damaging the primary cultured cortical neurons derived from embryonic mice. J Neurosci Res 89:552–561.
Lafuente JV, Argandoña EG, Mitre B (2006) VEGFR-2 expression in brain injury: its distribution related to brain–blood barrier markers. J Neural Transm 113:487–496.
Lattanzi W, Corvino V, Di Maria V, Michetti F, Geloso MC (2013) Gene expression profiling as a tool to investigate the molecular machinery activated during hippocampal neurodegeneration induced by trimethyltin (TMT) administration. Int J Mol Sci 14:16817–16835.
Lee DJ, Hsu MS, Seldin MM, Arellano JL, Binder DK (2012) Decreased expression of the glial water channel aquaporin-4 in the intrahippocampal kainic acid model of epileptogenesis. Exp Neurol 235:246–255.
Lee HT, Chang YC, Tu YF, Huang CC (2009) VEGF-A/VEGFR-2 signaling leading to cAMP response element-binding protein phosphorylation is a shared pathway underlying the protective effect of preconditioning on neurons and endothelial cells. J Neurosci 29:4356–4368.
Licht T, Keshet E (2013) Delineating multiple functions of VEGF-A in the adult brain. Cell Mol Life Sci 70:1727–1737.
Little AR, Benkovic SA, Miller DB, O'Callaghan JP (2002) Chemically induced neuronal damage and gliosis: enhanced expression of the proinflammatory chemokine, monocyte chemoattractant protein (MCP)-1, without a corresponding increase in proinflammatory cytokines(1). Neuroscience 115:307–320.
Little AR, Miller DB, Li S, Kashon ML, O'Callaghan JP (2012) Trimethyltin-induced neurotoxicity: gene expression pathway analysis, q-RT-PCR and immunoblotting reveal early effects associated with hippocampal damage and gliosis. Neurotoxicol Teratol 34:72–82.
Lo AC, Chen AY, Hung VK, Yaw LP, Fung MK, Ho MC, Tsang MC, Chung SS, Chung SK (2005) Endothelin-1 overexpression leads to further water accumulation and brain edema after middle cerebral artery occlusion via aquaporin 4 expression in astrocytic end-feet. J Cereb Blood Flow Metab 25:998–1011.
Lowry OH, Rosebrough NJ, Farr AL, Randall RJ (1951) Protein measurement with the Folin phenol reagent. J Biol Chem 193:265–275.
Mackenzie F, Ruhrberg C (2012) Diverse roles for VEGF-A in the nervous system. Development 139:1371–1380.
McCann MJ, O'Callaghan JP, Martin PM, Bertram T, Streit WJ (1996) Differential activation of microglia and astrocytes following trimethyltin-induced neurodegeneration. Neuroscience 72:273–281.
Michalak Z, Lebrun A, Di Miceli M, Rousset MC, Crespel A, Coubes P, Henshall DC, Lerner-Natoli M, Rigau V (2012) IgG leakage may contribute to neuronal dysfunction in drug-refractory epilepsies with blood–brain barrier disruption. J Neuropathol Exp Neurol 71:826–838.
Michalak Z, Sano T, Engel T, Miller-Delaney SF, Lerner-Natoli M, Henshall DC (2013) Spatio-temporally restricted blood–brain barrier disruption after intra-amygdala kainic acid-induced status epilepticus in mice. Epilepsy Res 103:167–179.
Michalski D, Grosche J, Pelz J, Schneider D, Weise C, Bauer U, Kacza J, Gärtner U, Hobohm C, Härtig W (2010) A novel quantification of blood–brain barrier damage and histochemical typing after embolic stroke in rats. Brain Res 1359:186–200.
Morin-Brureau M, Lebrun A, Rousset MC, Fagni L, Bockaert J, de Bock F, Lerner-Natoli M (2011) Epileptiform activity induces vascular remodeling and zonula occludens 1 downregulation in organotypic hippocampal cultures: role of VEGF signaling pathways. J Neurosci 31:10677–10688.
Nagelhus EA, Mathiisen TM, Ottersen OP (2004) Aquaporin-4 in the central nervous system: cellular and subcellular distribution and coexpression with KIR4.1. Neuroscience 129:905–913.
Nagelhus EA, Ottersen OP (2013) Physiological roles of aquaporin-4 in brain. Physiol Rev 93:1543–1562.
Ndode-Ekane XE, Hayward N, Gröhn O, Pitkänen A (2010) Vascular changes in epilepsy: functional consequences and association with network plasticity in pilocarpine-induced experimental epilepsy. Neuroscience 166:312–332.
Nesic O, Lee J, Ye Z, Unabia GC, Rafati D, Hulsebosch CE, Perez-Polo JR (2006) Acute and chronic changes in aquaporin 4 expression after spinal cord injury. Neuroscience 143:779–792.
Nico B, Frigeri A, Nicchia GP, Corsi P, Ribatti D, Quondamatteo F, Herken R, Girolamo F, Marzullo A, Svelto M, Roncali L (2003) Severe alterations of endothelial and glial cells in the blood–brain barrier of dystrophic mdx mice. Glia 42:235–251.
Nico B, Ribatti D (2012) Morphofunctional aspects of the blood–brain barrier. Curr Drug Metab 13:50–60.
Nielsen S, Nagelhus EA, Amiry-Moghaddam M, Bourque C, Agre P, Ottersen OP (1997) Specialized membrane domains for water transport in glial cells: high-resolution immunogold cytochemistry of aquaporin-4 in rat brain. J Neurosci 17:171–180.
Nilsberth C, Kostyszyn B, Luthman J (2002) Changes in APP, PS1 and other factors related to Alzheimer's disease pathophysiology after trimethyltin-induced brain lesion in the rat. Neurotox Res 4:625–636.
Papadopoulos MC, Saadoun S, Binder DK, Manley GT, Krishna S, Verkman AS (2004) Molecular mechanisms of brain tumor edema. Neuroscience 129:1011–1020.
Papadopoulos MC, Verkman AS (2007) Aquaporin-4 and brain edema. Pediatr Nephrol 22:778–784.
Patel M, Ardelt BK, Yim GK, Isom GE (1990) Interaction of trimethyltin with hippocampal glutamate. Neurotoxicol 11:601–608.
Pavlaković G, Kane MD, Eyer CL, Kanthasamy A, Isom GE (1995) Activation of protein kinase c by trimethyltin: relevance to neurotoxicity. J Neurochem 65:2338–2343.
Pekny M, Nilsson M (2005) Astrocyte activation and reactive gliosis. Glia 50:427–434.
Proescholdt MA, Heiss JD, Walbridge S, Mühlhauser J, Capogrossi MC, Oldfield EH, Merrill MJ (1999) Vascular endothelial growth factor (VEGF) modulates vascular permeability and inflammation in rat brain. J Neuropathol Exp Neurol 58:613–627.
Piacentini R, Gangitano C, Ceccariglia S, Del Fà A, Azzena GB, Michetti F, Grassi C (2008) Dysregulation of intracellular calcium homeostasis is responsible for neuronal death in an experimental model of selective hippocampal degeneration induced by trimethyltin. J Neurochem 105:2109–2121.
Qu M, Zhou Z, Chen C, Li M, Pei L, Chu F, Yang J, Wang Y, Li L, Liu C, Zhang L, Zhang G, Yu Z, Wang D (2011) Lycopene protects against trimethyltin-induced neurotoxicity in primary cultured rat hippocampal neurons by inhibiting the mitochondrial apoptotic pathway. Neurochem Int 59:1095–1103.
Rash JE, Yasumura T, Hudson CS, Agre P, Nielsen S (1998) Direct immunogold labeling of aquaporin-4 in square arrays of astrocyte and ependymocyte plasma membranes in rat brain and spinal cord. Proc Natl Acad Sci U S A 95:11981–11986.
Reali C, Scintu F, Pillai R, Donato R, Michetti F, Sogos V (2005) S100B counteracts effects of the neurotoxicant trimethyltin on astrocytes and microglia. J Neurosci Res 81:677–686.
Rigau V, Morin M, Rousset MC, de Bock F, Lebrun A, Coubes P, Picot MC, Baldy-Moulinier M, Bockaert J, Crespel A, Lerner-Natoli M (2007) Angiogenesis is associated with blood–brain barrier permeability in temporal lobe epilepsy. Brain 130:1942–1956.
Röhl C, Sievers J (2005) Microglia is activated by astrocytes in trimethyltin intoxication. Toxicol Appl Pharmacol 204:36–45.
Ryu JK, McLarnon JG (2009) A leaky blood–brain barrier, fibrinogen infiltration and microglial reactivity in inflamed Alzheimer's disease brain. J Cell Mol Med 13:2911–2925.
Saadoun S, Papadopoulos MC, Davies DC, Krishna S, Bell BA (2002) Aquaporin-4 expression is increased in oedematous

human brain tumours. J Neurol Neurosurg Psychiatry 72:262–265.
Saadoun S, Papadopoulos MC (2010) Aquaporin-4 in brain and spinal cord oedema. Neuroscience 168:1036–1046.
Scharfman HE, Binder DK (2013) Aquaporin-4 water channels and synaptic plasticity in the hippocampus. Neurochem Int [Epub ahead of print].
Seifert G, Schilling K, Steinhäuser C (2006) Astrocyte dysfunction in neurological disorders: a molecular perspective. Nat Rev Neurosci 7:194–206.
Shin EJ, Suh SK, Lim YK, Jhoo WK, Hjelle OP, Ottersen OP, Shin CY, Ko KH, Kim WK, Kim DS, Chun W, Ali S, Kim HC (2005) Ascorbate attenuates trimethyltin-induced oxidative burden and neuronal degeneration in the rat hippocampus by maintaining glutathione homeostasis. Neuroscience 133:715–727.
Simard M, Nedergaard M (2004) The neurobiology of glia in the context of water and ion homeostasis. Neuroscience 129:877–896.
Steinhäuser C, Seifert G (2002) Glial membrane channels and receptors in epilepsy: impact for generation and spread of seizure activity. Eur J Pharmacol 447:227–237.
Sun L, Yang L, Xu YW, Liang H, Han J, Zhao RJ, Cheng Y (2012) Neuroprotection of hydroxysafflor yellow A in the transient focal ischemia: inhibition of protein oxidation/nitration, 12/15-lipoxygenase and blood–brain barrier disruption. Brain Res 1473:227–235.
Tait MJ, Saadoun S, Bell BA, Papadopoulos MC (2008) Water movements in the brain: role of aquaporins. Trends Neurosci 31:37–43.
Taniguchi M, Yamashita T, Kumura E, Tamatani M, Kobayashi A, Yokawa T, Maruno M, Kato A, Ohnishi T, Kohmura E, Tohyama M, Yoshimine T (2000) Induction of aquaporin-4 water channel mRNA after focal cerebral ischemia in rat. Brain Res Mol Brain Res 78:131–137.
Tian GF, Azmi H, Takano T, Xu Q, Peng W, Lin J, Oberheim N, Lou N, Wang X, Zielke HR, Kang J, Nedergaard M (2005) An astrocytic basis of epilepsy. Nat Med 11:973–981.
Vajda Z, Promeneur D, Dóczi T, Sulyok E, Frøkiaer J, Ottersen OP, Nielsen S (2000) Increased aquaporin-4 immunoreactivity in rat brain in response to systemic hyponatremia. Biochem Biophys Res Commun 270:495–503.
van Bruggen N, Thibodeaux H, Palmer JT, Lee WP, Fu L, Cairns B, Tumas D, Gerlai R, Williams SP, van Lookeren Campagne M, Ferrara N (1999) VEGF antagonism reduces edema formation and tissue damage after ischemia/reperfusion injury in the mouse brain. J Clin Invest 104:1613–1620.
Verkman AS (2002) Aquaporin water channels and endothelial cell function. J Anat 200:617–627.
Verkman AS (2005) More than just water channels: unexpected cellular roles of aquaporins. J Cell Sci 118:3225–3232.
Vizuete ML, Venero JL, Vargas C, Ilundáin AA, Echevarría M, Machado A, Cano J (1999) Differential upregulation of aquaporin-4 mRNA expression in reactive astrocytes after brain injury: potential role in brain edema. Neurobiol Dis 6:245–258.
Warth A, Simon P, Capper D, Goeppert B, Tabatabai G, Herzog H, Dietz K, Stubenvoll F, Ajaaj R, Becker R, Weller M, Meyermann R, Wolburg H, Mittelbronn M (2007) Expression pattern of the water channel aquaporin-4 in human gliomas is associated with blood–brain barrier disturbance but not with patient survival. J Neurosci Res 85:1336–1346.
Zhang ZG, Zhang L, Jiang Q, Zhang R, Davies K, Powers C, Bruggen Nv, Chopp M (2000) VEGF enhances angiogenesis and promotes blood–brain barrier leakage in the ischemic brain. J Clin Invest 106:829–838.
Zlokovic BV (2008) The blood–brain barrier in health and chronic neurodegenerative disorders. Neuron 57:178–201.

(Accepted 21 May 2014)
(Available online 6 June 2014)